Journal of Industrial Microbiology & Biotechnology (2019) 46:1505–1516
https://doi.org/10.1007/s10295-019-02214-1

METABOLIC ENGINEERING AND SYNTHETIC BIOLOGY - ORIGINAL PAPER

Combinatorial expression of different β-carotene hydroxylases and ketolases in *Escherichia coli* for increased astaxanthin production

Yuanqing Wu[1] · Panpan Yan[1] · Xuewei Liu[1] · Zhiwen Wang[1] · Ya-Jie Tang[2,3] · Tao Chen[1] · Xueming Zhao[1]

Received: 12 March 2019 / Accepted: 4 July 2019 / Published online: 11 July 2019

Abstract

In natural produced bacteria, β-carotene hydroxylase (CrtZ) and β-carotene ketolase (CrtW) convert β-carotene into astaxanthin. To increase astaxanthin production in heterologous strain, simple and effective strategies based on the co-expression of CrtZ and CrtW were applied in *E. coli*. First, nine artificial operons containing *crtZ* and *crtW* genes from different sources were constructed and, respectively, introduced into *E. coli* ZF237T, a β-carotene producing host. Among the nine resulting strains, five accumulated detectable amounts of astaxanthin ranging from 0.49 to 8.07 mg/L. Subsequently, the protein fusion CrtZ to CrtW using optimized peptide linkers further increased the astaxanthin production. Strains expressing fusion proteins with CrtZ rather than CrtW attached to the N-terminus accumulated much more astaxanthin. The astaxanthin production of the best strain ZF237T/$CrtZ_{As}$-$(GS)_1$-W_{Bs} was 127.6% and 40.2% higher than that of strains ZF237T/$crtZ_{As}W_{Bs}$ and ZF237T/$crtZ_{Bs}W_{Ps}$, respectively. The strategies depicted here also will be useful for the heterologous production of other natural products.

Keywords Astaxanthin · Combinatorial expression · Artificial operon · Fusion protein · Bifunctional enzymes

Introduction

Astaxanthin (3,3′-dihydroxy-β,β-carotene-4,4′-dione) is an important natural red–orange pigment with one of the highest antioxidative activities. It is widely used in pharmaceuticals, cosmetics, health products, food and beverage due to its various health benefits [15]. Usually, the biosynthetic pathway of astaxanthin is artificially divided into two parts, the biosynthesis of β-carotene and astaxanthin formation (Fig. 1). In bacteria, the reactions from β-carotene to astaxanthin are normally catalyzed by two oxygenases, but the pathways vary. The β-carotene hydroxylase (CrtZ) is involved in hydroxyl introducing at positions C-3 and C-3′, while the ketolase (CrtW) is responsible for keto group formation at positions C-4 and C-4′ [26]. The Misawa group isolated and determined the functions of the gene cluster involved in astaxanthin production in *Agrobacterium aurantiacum* and identified the astaxanthin biosynthesis pathway at the level of individual genes for the first time [28]. Later they found that the astaxanthin biosynthesis enzymes from bacteria and *Haematococcus pluvialis* are bifunctional and have different substrates preference [10, 11]. In addition, Scaife et al. investigated 12 genes encoding β-carotene ketolases and 4 encoding β-carotene hydroxylases from 5 cyanobacterial species in vivo and reached the same conclusion [35]. In addition to the substrate preference, both CrtZ and CrtW can simultaneously catalyze the oxygenation of the respective positions on one or both of the β-ionone rings, which makes it difficult to identity the main reaction

Electronic supplementary material The online version of this article (https://doi.org/10.1007/s10295-019-02214-1) contains supplementary material, which is available to authorized users.

✉ Tao Chen
chentao@tju.edu.cn

[1] Frontier Science Center for Synthetic Biology and Key Laboratory of Systems Bioengineering (Ministry of Education), SynBio Research Platform, Collaborative Innovation Center of Chemical Science and Engineering (Tianjin), School of Chemical Engineering and Technology, Tianjin University, Tianjin 300072, People's Republic of China

[2] State Key Laboratory of Microbial Technology, Shandong University, Qingdao 266237, People's Republic of China

[3] Key Laboratory of Fermentation Engineering (Ministry of Education), Hubei Key Laboratory of Industrial Microbiology, Hubei Provincial Cooperative Innovation Center of Industrial Fermentation, Hubei University of Technology, Wuhan 430068, People's Republic of China

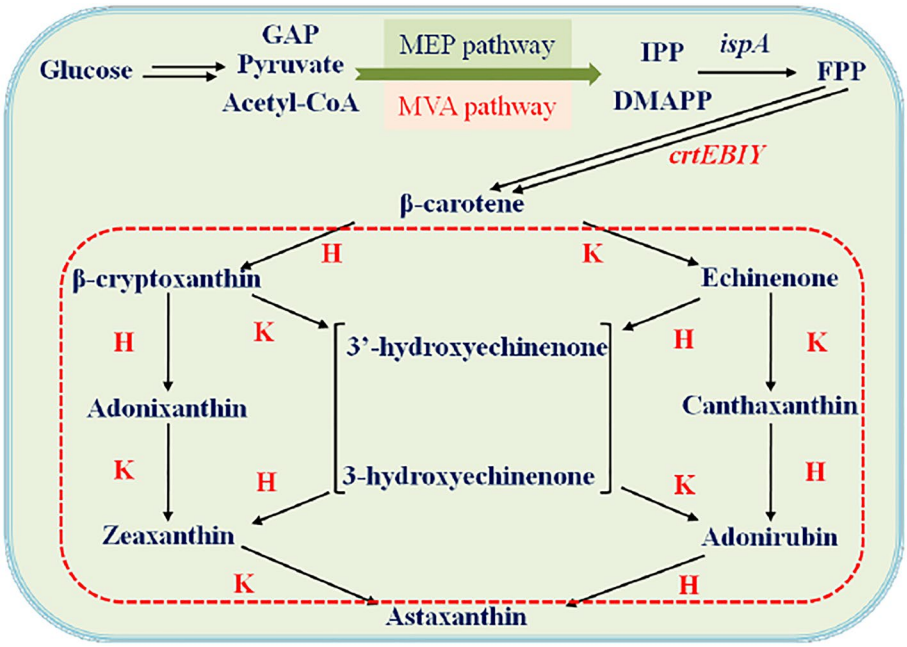

Fig. 1 The biosynthetic pathway of astaxanthin in engineered *E. coli*. The biosynthetic pathway was artificially divided into two parts, the biosynthesis of β-carotene and astaxanthin formation. Heterologous pathways are shown in red. *GAP* glyceraldehyde-3P, *IPP* isopentenyl pyrophosphate, *DMAPP* dimethylallyl pyrophosphate, *FPP* farnesyl pyrophosphate, *MEP* pathway 2-C-methyl-D-erythritol-4-phosphate pathway, *MVA* pathway mevalonate pathway, *ispA* FPP synthase, *crtE* GGPP synthase, *crtB* phytoene synthase, *crtI* phytoene desaturase, *crtY* lycopene cyclase, *H* β-carotene hydroxylase, *K* β-carotene ketolase (color figure online)

in natural astaxanthin producers that possess the two oxygenases. Consequently, conversion of β-carotene into astaxanthin is accomplished via multiple intermediate products (Fig. 1).

In recent years, some representative microbiological systems including heterologous strains of *E. coli* [23, 25, 32, 38, 40], *Saccharomyces cerevisiae* [16, 41, 42] and *Corynebacterium glutamicum* [14] have been engineered to accumulate astaxanthin by various metabolic engineering strategies. The strategies which were used individually or jointly include enzyme quarrying, promoter control, optimization of ribosome binding sites and codon usage, protein engineering, discovery of new targets and gene copy number regulation. Among these studies, some engineered *E. coli* strains with potential for industrial applications were constructed. For example, *E. coli* strain E [40] and WLGB-RPP (pAX15) [32] produced astaxanthin titers of 320 mg/L and 332.23 mg/L in fed-batch fermentation, respectively. In these engineered strains, the genes involved in astaxanthin biosynthesis were introduced by a controlled arrangement of reactions or dual expression vectors. In natural producers, the genes involved in astaxanthin biosynthesis are present on the genome in form of gene cluster [30]. To our knowledge, there are only few reports about regulating astaxanthin accumulation through the combinatorial co-expression of CrtZ and CrtW within an expression cassette in engineered strains.

In this work, we used simple and effective combinatorial strategies to optimize the heterologous astaxanthin biosynthesis pathway in *E. coli*. The *crtZ* and *crtW* genes from different sources were combined and co-expressed. The co-expression of the *crtZ* gene from *Brevundimonas* sp. SD212 and *crtW* gene from *Paracoccus* sp. N81106 yielded the best astaxanthin accumulation. Based on the improved combinations, a series of fusion proteins were constructed and the astaxanthin production was significantly enhanced by expressing a CrtZ-W fusion protein. Finally, the astaxanthin production and content were further increased via carbon resource optimization.

Materials and methods

Strains, media and culture conditions

E. coli DH5α was used to construct recombinant plasmids and *E. coli* strain ZF237T was used as host for astaxanthin production [20]. LB medium [10 g tryptone, 5 g yeast extract, 10 g sodium chloride per liter with or without 1.5% (m/v) agar] containing 20 mg/L of ampicillin was used for plasmids construction. During plasmids construction, cultures were grown in a rotary shaker at 220 rpm and 37 °C or statically at 37 °C. 2×YT medium (16 g tryptone, 10 g yeast extract, 5 g sodium chloride per liter) was used for fermentation in shake flasks. All strains are listed in Table S1.

Plasmid construction

All DNA manipulation procedures were implemented according to standard procedures [34]. Restriction enzyme digestion and overlap extension PCR [13] were performed to construct designed recombinant plasmids. All plasmids and primers used in this study are listed in Tables S1 and S2. The *crtZ* genes from *Paracoccus* sp. N81106 (*A. aurantiacum*), *Alcaligenes* sp. strain PC-1 and *Brevundimonas* sp. SD212,

and the *crtW* genes from *Paracoccus* sp. N81106, *Brevundimonas* sp. SD212 and *Nostoc* sp. PCC7120 were codon optimized and chemically synthesized by Wuhan GeneCreate biological engineering Co. LTD (China) and cloned into plasmid pUC57. To construct the nine artificial expression operons, the *crtZ* gene was amplified from the plasmid pUC57-Z using the primers Z-5′-EcoRI/Z-3′-BamHI with the primer Z-5′-EcoRI containing the sequences of promoter J23119 and RBS apFAB917. Similarly, the *crtW* gene was amplified from the plasmid pUC57-W using the primers W-5′-BamHI/W-3′-HindIII with the primer W-5′-BamHI containing the sequences of the RBS apFAB916. The purified *crtZ* gene fragment was digested with *Eco*R I and *Bam*H I and inserted between the corresponding sites of plasmid p5C. Subsequently, the *crtW* gene fragment was located at the *Bam*H I/*Hin*d III sites of plasmid p5C-Z after digestion with *Bam*H I and *Hin*d III. To construct CrtZ-W fusion proteins, the stop codon of the *crtZ* gene was removed and the fusion gene was inserted into plasmid p5C via enzyme digestion-ligation after splicing by overlap-extension PCR using the primers CrtZ-5′-EcoRI/CrtW-3′-HindIII. The CrtW-Z fusion proteins were constructed analogously. The linkers of different lengths, $(Gly–Ser–Gly)_x$ ($x=1$, 2, 3, or 4), or $(Gly–Ser)_y$ ($y=1$, 2, 3, 4, or 5), which were introduced between open reading frames, were incorporated into primers as overlap sequences. The codons of linkers for *E. coli* were chosen using the Codon Adaptation Tool (JCAT) (http://www.jcat.de/). All recombinant plasmids were verified through sequencing by GENEWIZ, Inc (Beijing, China).

Quantitative real-time PCR

Quantitative real-time PCR was applied to measure the transcriptional levels of genes in the engineered strains. Cells were collected after 48 h of shake-flask fermentation. Total RNA extraction and cDNA synthesis were the same as described previously [21]. Quantitative PCR was conducted using the ABI7500 Real-Time PCR kit (Applied Biosystems, USA) with SYBR® Premix Ex Taq™ II (Tli RNaseH Plus) and ROX plus (TaKaRa, Dalian, China). The primers used for qPCR are listed in Table S2. The data were quantified using the $2^{-\Delta\Delta CT}$ method as described before [22]. The *rrsA* gene was used as internal standard for normalization, and three biological replicates and sample repetitions were performed.

Homology modeling

The homology-based models of *Alcaligenes* sp. strain PC-1 CrtZ, *Brevundimonas* sp. SD212 CrtW, as well as the fusion proteins $CrtW_{As}$-Z_{Bs} and $CrtZ_{Bs}$-W_{As} were modeled using I-TASSER (https://zhanglab.ccmb.med.umich.edu/I-TASSER/) [37]. The specific operations were described by Roy et al. [33]. To the best of our knowledge, there are no crystal structures of β-carotene hydroxylases and β-carotene ketolases in the PDB library, so we chose model 1 from each prediction output according to the C-score and TM-score, which indicate prediction reliability and alignment identity, respectively.

Shake-flask fermentation

The engineered *E. coli* strains were cultured in 5 mL LB medium with appropriate antibiotics at 30 °C overnight in a rotary shaker (220 rpm). The liquid cultures were then transferred to 500 mL flasks containing 100 mL of 2 × YT medium with 10 g/L glucose or 10 g/L other carbon source for fermentation optimization and appropriate antibiotics (20 mg/L for ampicillin and 10 m/L for kanamycin) to an initial OD_{600} of about 0.04 and cultivated under the same conditions for 96 h.

Analytical methods

Intracellular carotenoids were extracted as described previously [20]. The extract was analyzed by high-performance liquid chromatography (HITACHI Primaide, Japan) equipped with a HyPURITY C18 column (150 × 4.6 mm, 5 µm, Thermo Fisher Scientific, Inc., USA) to determine the concentration of astaxanthin and identify other carotenoids. The analyte signals were detected at 470 nm. Solvent A consisting of 90% aqueous acetonitrile (HPLC grade) and solvent B consisting of methyl alcohol-isopropyl alcohol (3:2, v/v, HPLC grade) were used as mobile phase at a flow rate of 1.0 mL/min. A 35-min gradient program was used to elute the analytes as follows: 100–10% solvent A (0–15 min), 10% solvent A (15–30 min), 10–100% solvent A (30–35 min) [42]. The authentic carotenoid standards and their retention times were as follows: astaxanthin (≥ 97%, Sigma-Aldrich, USA), 7.1 min; zeaxanthin (≥ 95%, Sigma-Aldrich, USA), 9.1 min; canthaxanthin (≥ 95%, Sigma-Aldrich, USA), 11.7 min; echinenone (≥ 95%, Sigma-Aldrich, USA), 17.6 min; lycopene (≥ 98%, Sigma-Aldrich, USA), 20.9 min; β-carotene (≥ 95%, Sigma-Aldrich, USA), 22.8 min. The OD_{600} was used as cell growth indicator. For *E. coli*, the OD_{600} and dry cell weight (DCW) had the following conversion relation: 1 OD_{600} = 0.323 g DCW/L. The concentration of glucose was determined using an SBA-40C biosensor analyzer (Institute of Microbiology, Shandong, China). The concentration of glycerol was measured by HPLC (HITACHI Primaide, Japan) equipped with an Aminex HPX-87H column (300 × 7.8 mm, Bio-Rad, Inc., USA). The mobile phase was 5 mM H_2SO_4 with flow rate of 0.5 mL/min, and the column temperature was 50 °C.

Results

Design of the β-carotene hydroxylase and -ketolase coexpression system

Previous studies revealed that CrtZ can efficiently convert β-carotene into zeaxanthin, as well as that the main product of zeaxanthin conversion by CrtW is astaxanthin in *E. coli* [7, 8]. Transcription and translation are generally coupled in bacteria, including *E. coli*, and the sequence of translation is related to the sequence of genes in polycistronic operons [24]. The *E. coli* strain ZF237T, which harbors an artificial *crtEBIY* operon and another 15 modified genes in its genome, is a β-carotene overproducing engineered strain [20]. To engineer it to produce astaxanthin, *crtZ–crtW* expression cassette was designed. The transcription of the cassette was controlled by the Anderson promoter J23119 instead of an IPTG-induced promoter, as IPTG was unfavorable for lycopene accumulation in *E. coli* [17]. The RBS apFAB917 was used for *crtZ* and apFAB916 for *crtW*. The combinations of the promoter and the RBSs have high mRNA and high protein levels [18]. The cassette was assembled through enzymatic digestion-ligation and inserted into the low copy number plasmid p5C (Fig. 2a) to avoid a possible severe metabolic burden on the host.

Construction and expression of 9 cassettes in vivo

It has been discovered that there are many different β-carotene hydroxylases and -ketolases in nature. This facilitates isoenzyme selection to regulate astaxanthin production. Previous endeavors succeeded in increasing astaxanthin production by utilizing different hydroxylases and ketolases from various origins [23, 36, 40]. The β-carotene hydroxylases from *Paracoccus* sp. N81106 ($CrtZ_{Ps}$), *Alcaligenes* sp. strain PC-1 ($CrtZ_{As}$) and *Brevundimonas* sp. SD212 ($CrtZ_{Bs}$), and the β-carotene ketolases CrtW from *Paracoccus* sp. N81106 ($CrtW_{Ps}$), *Brevundimonas* sp. SD212 ($CrtW_{Bs}$) and *Nostoc* sp. PCC7120 ($CrtW_{Ns}$) were chosen to construct expression cassettes due to their higher substrate

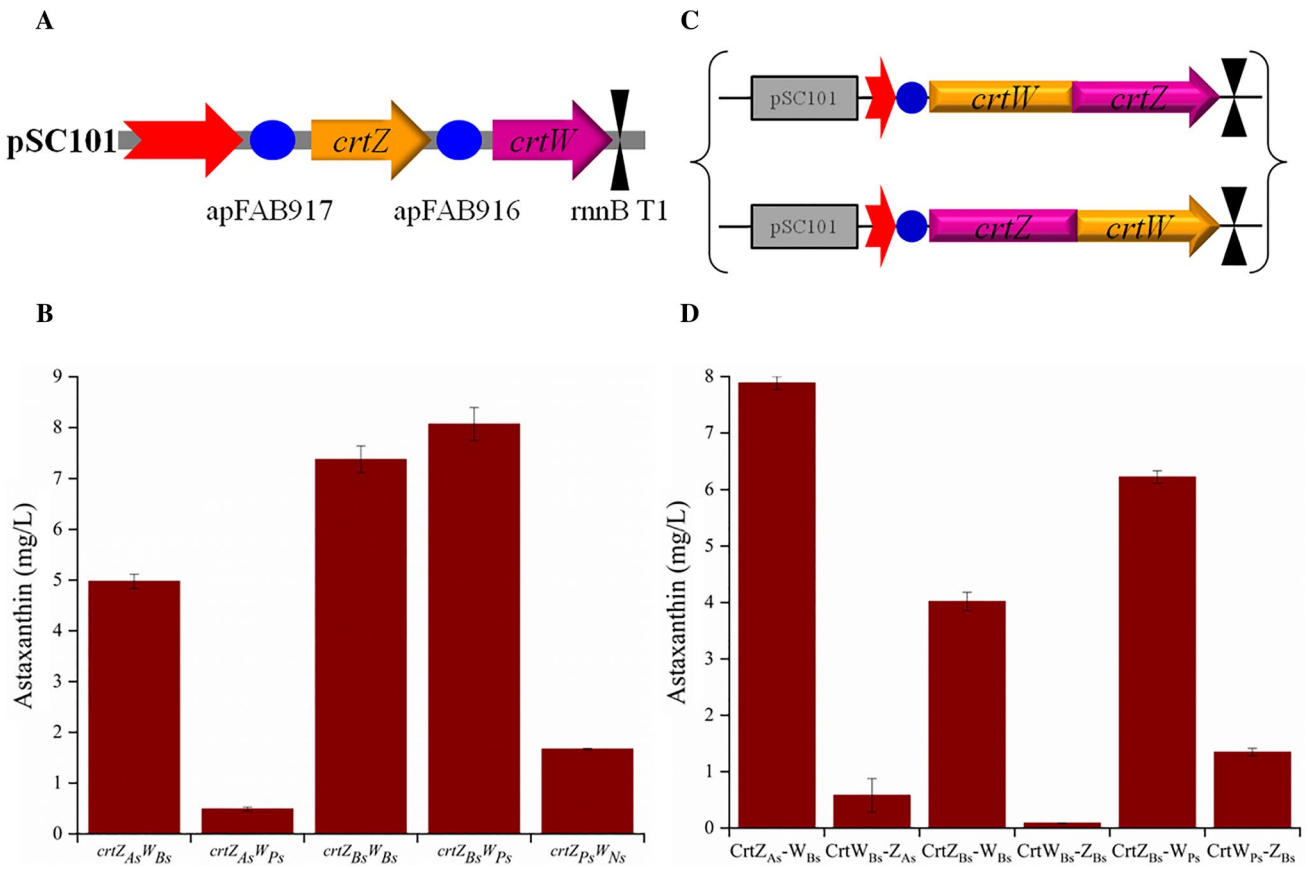

Fig. 2 Astaxanthin production by *E. coli* ZF237T derivatives expressing various artificial operons and fusion proteins. **a**, **c** The designs of different operons and fusion proteins. The swallowtail arrow denotes the promoter J23119, the blue solid circle denotes the RBS apFAB917. **b** The production of astaxanthin by strains expressing various operons, and **d** CrtW-Z and CrtZ-W fusion proteins (color figure online)

conversion efficiencies in vivo [7, 8, 35]. The three *crtZ* genes were combined with the three *crtW* genes according to the design mentioned above so that a total of nine *crtZW* expression plasmids were constructed and transferred into strain ZF237T.

All the colonies harboring any of the nikne different *crtZW* expression plasmids showed red color after cultivation for 24 h on LB agar plates, and their carotenoid composition was analyzed. All strains accumulated lycopene, but only five accumulated detectable amounts of astaxanthin after 96 h of fermentation (Table 1). As shown in Fig. 2b, the astaxanthin production of strains ZF237T/$crtZ_{As}W_{Ps}$ and ZF237T/$crtZ_{Ps}W_{Ns}$ was less than 2 mg/L, while the strains ZF237T/$crtZ_{As}W_{Bs}$, ZF237T/$crtZ_{Bs}W_{Bs}$ and ZF237T/$crtZ_{Bs}W_{Ps}$ produced 4.97, 7.38 and 8.07 mg/L of astaxanthin, respectively. The astaxanthin production of strain ZF237T/$crtZ_{Bs}W_{Ps}$ was 16.5 times that of strain ZF237T/$crtZ_{As}W_{Ps}$. However, among the four non-astaxanthin-accumulating strains, the product distribution differed greatly (Table 1). For example, strain ZF237T/$crtZ_{Ps}W_{Bs}$ accumulated canthaxanthin without detectable amount of zeaxanthin, while strain ZF237T/$crtZ_{Bs}W_{Ns}$ accumulated zeaxanthin without detectable amounts of canthaxanthin.

Construction of fusion proteins

In *Xanthophyllomyces dendrorhous*, a single chromosomally encoded P450 protein, CrtS, directly converts β-carotene into astaxanthin using CrtR as electron donor [2]. However, the expression of P450 enzymes involved in terpenoids biosynthesis in *E. coli* is still very challenging [3, 5]. The genetic fusion of proteins was originally developed for protein expression/purification and was later adopted to enhance metabolic fluxes by facilitating substrate channeling [1, 43]. Two broad classes of fusion proteins are usually designed by changing the location of an enzyme. To produce astaxanthin from β-carotene more efficiently, three CrtZ-W and three CrtW-Z fusion proteins were designed and constructed based on the three combinations that showed higher astaxanthin production (Fig. 2b) when expressed independently, $crtZ_{As}W_{Bs}$, $crtZ_{Bs}W_{Bs}$ and $crtZ_{Bs}W_{Ps}$. The expression of the fusion proteins was controlled by the constitutive promoter J23119 and RBS apFAB917. The expression cassettes encoding these fusion proteins were also inserted into plasmid p5C after assembly (Fig. 2c).

The six fusion proteins comprised three pairs, $CrtZ_{As}$-W_{Bs} and $CrtW_{Bs}$-Z_{As}, $CrtZ_{Bs}$-W_{Bs} and $CrtW_{Bs}$-Z_{Bs}, $CrtZ_{Bs}$-W_{Ps} and $CrtW_{Ps}$-Z_{Bs}, which were fused directly (Fig. 2c). The fusion protein expression plasmids were, respectively, introduced into strain ZF237T and the six resulting strains were cultivated in shake flasks. The astaxanthin concentrations were determined after 96 h of fermentation. Unexpectedly, the strains expressing CrtZ-W variants produced much more astaxanthin than the corresponding CrtW-Z expressing strains (Fig. 2d). The maximum difference of astaxanthin production was up to 45.9-fold within fusion protein pair ($CrtZ_{Bs}$-W_{Bs} versus $CrtW_{Bs}$-Z_{Bs}). The results indicate that fusion proteins with CrtZ attached to the N-terminus are better for astaxanthin production. ZF237T/$CrtZ_{As}$-W_{Bs} produced 7.89 mg/L astaxanthin, which was 58.5% higher than the corresponding non-fusion protein expressing strain ZF237T/$crtZ_{As}W_{Bs}$. However, strains ZF237T/$CrtZ_{Bs}$-W_{Bs} and ZF237T/$CrtZ_{Bs}$-W_{Ps} produced 4.02 mg/L and 6.22 mg/L of astaxanthin, respectively, both of which were much lower than those of the corresponding non-fusion protein expressing strains (ZF237T/$crtZ_{Bs}W_{Bs}$ and ZF237T/$crtZ_{Bs}W_{Ps}$) (Fig. 2b, d). In addition, the production of astaxanthin produced by strain ZF237T/$CrtZ_{As}$-W_{Bs} was 2.2% lower than that of strain ZF237T/$crtZ_{Bs}W_{Ps}$. We, therefore, failed to increase astaxanthin production by fusing *crtZ and crtW*

Table 1 Carotenoids produced by different strains derived from ZF237T expressing operons containing *crtW* and *crtZ* genes from different sources

Operon	Astaxanthin (%)	Echinenone (%)	Canthaxanthin (%)	Zeaxanthin (%)	Lycopene (%)	β-Carotene (%)
$crtZ_{As}W_{Bs}$	41.68	0.00	0.00	7.81	50.51	0.00
$crtZ_{As}W_{Ps}$	8.34	0.00	7.19	32.71	45.49	6.26
$crtZ_{As}W_{Ns}$	0.00	8.99	25.94	0.00	9.83	55.24
$crtZ_{Bs}W_{Bs}$	63.42	5.63	3.76	15.90	11.29	0.00
$crtZ_{Bs}W_{Ps}$	60.20	3.71	4.11	16.84	15.14	0.00
$crtZ_{Bs}W_{Ns}$	0.00	0.00	0.00	84.41	15.59	0.00
$crtZ_{Ps}W_{Bs}$	0.00	8.10	71.35	0.00	20.55	0.00
$crtZ_{Ps}W_{Ps}$	0.00	3.93	72.03	0.00	17.96	6.08
$crtZ_{Ps}W_{Ns}$	6.88	10.57	2.22	0.00	4.08	76.25

The percentages were the ratios of peak area of HPLC. The data in table only indicated the carotenoids detected, and the same as Table 2. Although there is no relationship between the percentages and concentration of different carotenoids produced by strains, there is a linear relationship between the percentage and concentration of the same carotenoids

directly, which might be due to the lack of a linker between the two folding units.

Application of peptide linkers to increase astaxanthin production

As an important component of fusion proteins, linkers can significantly affect the biological function of fusion proteins. Previous reports demonstrated that flexible linkers are well-suited for engineering the fusion proteins with expected functions, and the length of flexible linkers was found to affect the catalytic efficiency of fusion proteins [12, 19]. The fusion protein $CrtZ_{As}$-W_{Bs} produced more astaxanthin than the other fusion proteins, so two types of flexible linkers with different lengths were introduced into it to further increase astaxanthin production.

The flexible linkers $(Gly\text{-}Ser\text{-}Gly)_x$ and $(Gly\text{-}Ser)_y$ are commonly used in the construction of fusion proteins [1, 6]. Here, two series of fusion proteins, $CrtZ_{As}$-$(Gly\text{-}Ser\text{-}Gly)_x$-$CrtW_{Bs}$ ($x = 1$, 2, 3 and 4) and $CrtZ_{As}$-$(Gly\text{-}Ser)_y$-$CrtW_{Bs}$ ($y = 1$, 2, 3, 4 and 5), were constructed, and the corresponding expression cassette was inserted in plasmid p5C, respectively. These fusion proteins were also expressed under the control of the promoter J23119 and the RBS apFAB917 (Fig. 3a). As shown in Fig. 3b, ZF237T/$CrtZ_{As}$-$(GS)_1$-W_{Bs}, ZF237T/$CrtZ_{As}$-$(GS)_2$-W_{Bs}, ZF237T/$CrtZ_{As}$-$(GSG)_2$-W_{Bs} and ZF237T/$CrtZ_{As}$-$(GSG)_3$-W_{Bs} produced 11.31 mg/L, 9.86 mg/L, 9.95 mg/L and 10.05 mg/L of astaxanthin, corresponding to an increase of 43.4%, 25.0%, 26.2% and 27.5% over the strain ZF237T/$CrtZ_{As}$-W_{Bs}, respectively. Moreover, the astaxanthin productions of the four strains increased by 40.2%, 22.2%, 23.4% and 24.6% compared with the non-fusion protein expressing strain ZF237T/$crtZ_{Bs}W_{Ps}$, respectively.

At the same time, the analysis of by-products showed that all strains accumulated the precursors, lycopene and β-carotene (Table 2). The strains expressing the fusion proteins $CrtZ_{As}$-$(GS)_1$-W_{Bs} and $CrtZ_{As}$-$(GS)_2$-W_{Bs} produced 3.71 mg/L and 2.93 mg/L of lycopene, respectively, which was lower than the corresponding value of strain ZF237T/$CrtZ_{As}$-W_{Bs} (5.78 mg/L), while strains $CrtZ_{As}$-$(GSG)_2$-W_{Bs} and $CrtZ_{As}$-$(GSG)_3$-W_{Bs} produced 6.52 mg/L and 5.30 mg/L of lycopene (Fig. 3c). The β-carotene production of the strains expressing the fusion proteins $CrtZ_{As}$-$(GS)_y$-W_{Bs} were lower than the corresponding value of strain ZF237T/$CrtZ_{As}$-W_{Bs} (5.92 mg/L), while the strains expressing the fusion proteins $CrtZ_{As}$-$(GSG)_1$-W_{Bs}, $CrtZ_{As}$-$(GSG)_2$-W_{Bs} and $CrtZ_{As}$-$(GSG)_4$-W_{Bs} produced 35.69, 8.60 and 33.57 mg/L of β-carotene, which was much higher than that of strain ZF237T/$CrtZ_{As}$-W_{Bs} (Fig. 3c). In addition, strains expressing the fusion proteins $CrtZ_{As}$-$(GS)_y$-W_{Bs} except for $CrtZ_{As}$-$(GS)_5$-W_{Bs} did not produce detectable amounts of canthaxanthin and echinenone, and the species of by-products increased with the increase of linker length, while strains expressing the fusion proteins $CrtZ_{As}$-$(GSG)_x$-W_{Bs} produced different intermediates with the varied length of linkers (Table 2). These results confirmed that the length of the peptide linkers $(GS)_x$ and $(GSG)_y$ can affect the catalytic efficiency of fusion proteins and thus influence by-product generation.

Optimization of the carbon source for strain ZF237T/$CrtZ_{As}$-$(GS)_1$-W_{Bs}

Glycerol has a significantly higher average degree of reduction per carbon ($C_3H_8O_3$: $\kappa = 4.67$) than sugars such as glucose ($C_6H_{12}O_6$: $\kappa = 4$) or xylose ($C_5H_{10}O_5$: $\kappa = 4$) [9]. This implies that glycerol can provide more reducing equivalents for astaxanthin biosynthesis, where two moles of NADPH are theoretically needed to converse one mole β-carotene into an equal amount of astaxanthin [10]. It is, therefore, perhaps not surprising that Park et al. demonstrated that glycerol is better for astaxanthin accumulation than glucose [32]. We, therefore, optimized the carbon source in the fermentation medium to increase astaxanthin production in shake flasks.

As shown in Fig. 4, when 10 g/L of glycerol was added into 2 × YT medium, the astaxanthin production was 23.71 mg/L and the intracellular content reached 4.67 mg/g DCW at the end of fermentation. These values were, respectively, 109.64% and 181.33% higher than those produced in 2 × YT medium containing 10 g/L glucose (1.66 mg/g DCW). This result verified that glycerol is more favorable than glucose for astaxanthin production. We also used a mixture of glycerol and glucose as carbon source. In host strain ZF237T, phosphotransferase system is inactivated, the expression of *galP* is enhanced and the genes involving acetate production are not inactivated [20]. To avoid metabolic overflow, 1% (m/v) of total carbon source was added into 2 × YT medium [27]. In view of that glycerol is better for astaxanthin production than glucose, the ratio of glycerol to glucose was set in a value no less than 1 in the mixtures. The analysis of astaxanthin production after 96 h of fermentation showed that the production decreased with the decrease of the ratio of glycerol to glucose (Fig. 4). When 8 g/L glycerol and 2 g/L glucose were added, the production of astaxanthin reached 26.16 mg/L and the content reached 5.18 mg/g DCW, which were comparable to the highest level in *E. coli* in shake flask reported previously [32]. In addition, the two values were 10.32% and 10.76% higher than those produced in 2 × YT medium containing 10 g/L glycerol, respectively. These results were consistent with previous report that appropriate ratio of glycerol to glucose within mixed carbon source was more beneficial for aromatic compounds' production in PTS^-Glc^+ *E. coli* strain [27]. The phenomena indicated that mixed carbon source

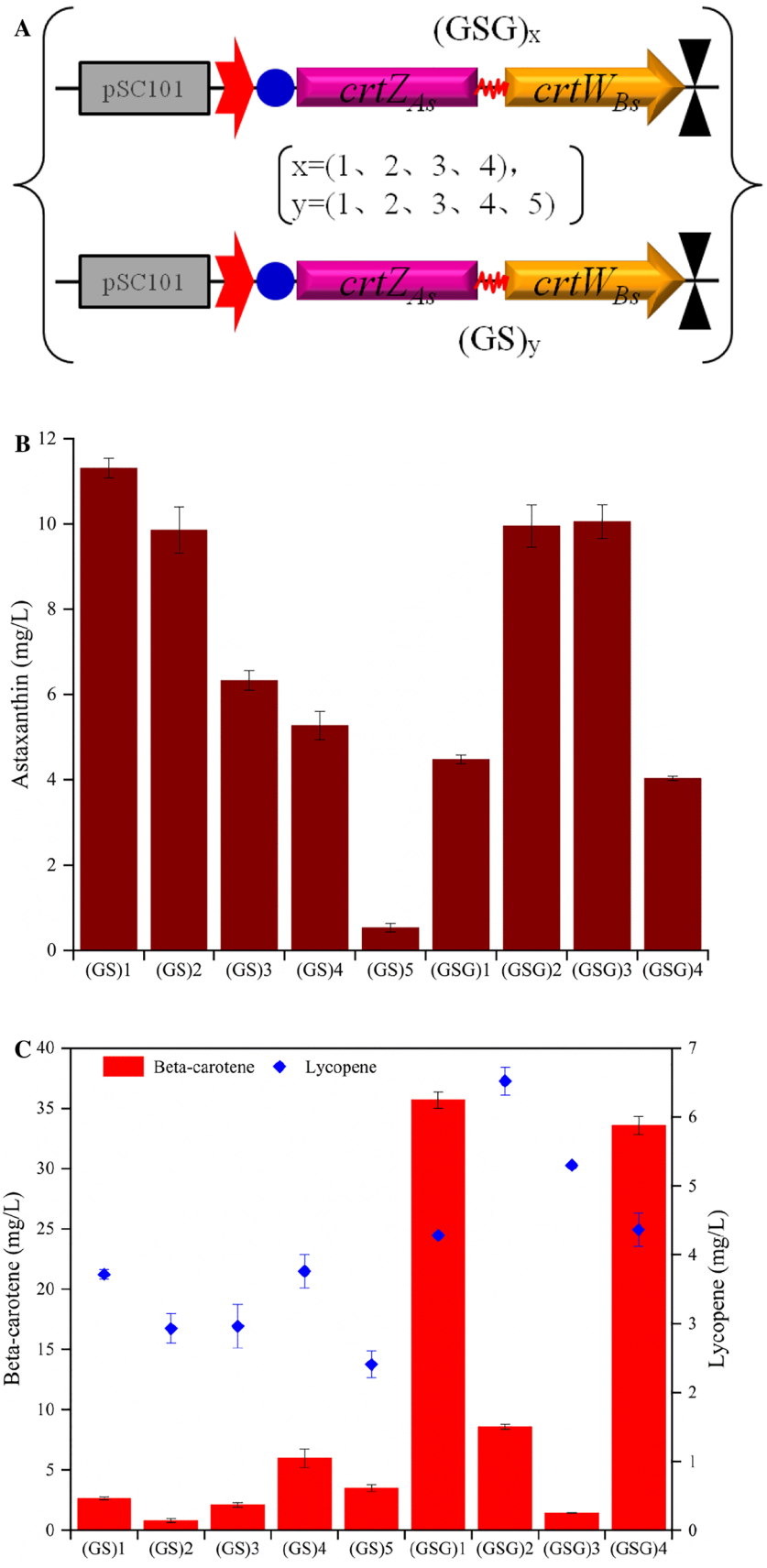

Fig. 3 Production of astaxanthin, lycopene and β-carotene by ZF237T-derived strains expressing different $CrtZ_{As}$-$(GS)_y$-W_{Bs} and $CrtZ_{As}$-$(GSG)_x$-W_{Bs} fusion proteins. **a** Designs for the introduction of peptide linkers. The swallowtail arrow denotes the promoter J23119, the blue solid circle denotes the RBS apFAB917. **b**, **c** The productions of astaxanthin, lycopene and β-carotene. The horizontal axis shows the abbreviations of different fusion proteins, i.e. (GS)1 and (GSG)1 denote fusion proteins $CrtZ_{As}$-$(GS)_1$-W_{Bs} and $CrtZ_{As}$-$(GSG)_1$-W_{Bs}, respectively (color figure online)

Table 2 Carotenoids produced by the ZF237T-derived strains expressing $CrtZ_{As}$-W_{Bs} formats fusion proteins with different linkers

Fusion proteins	Astaxanthin (%)	Zeaxanthin (%)	Canthaxanthin (%)	Echinenone (%)	Lycopene (%)	β-Carotene (%)
(GS)1	63.26	0.00	0.00	0.00	31.50	5.24
(GS)2	67.69	0.00	0.00	0.00	30.27	2.04
(GS)3	54.80	4.73	0.00	0.00	34.75	5.73
(GS)4	53.27	5.65	0.00	0.00	29.38	11.70
(GS)5	0.71	5.38	68.15	8.26	13.08	4.40
(GSG)1	17.12	0.00	0.00	5.75	25.25	51.88
(GSG)2	44.05	0.00	0.00	0.00	42.64	13.30
(GSG)3	50.18	4.55	3.72	0.00	39.14	2.41
(GSG)4	16.15	3.16	0.00	3.10	27.53	50.05

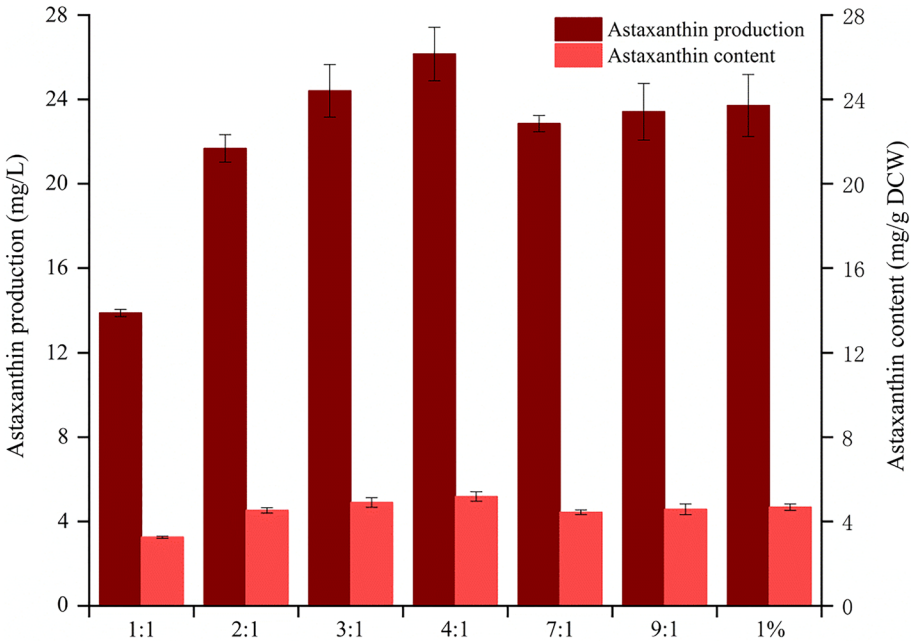

Fig. 4 The astaxanthin production of strain ZF237T/$CrtZ_{As}$-$(GS)_1$-W_{Bs} in 2×YT media with different carbon sources. Abscissa values represent the ratios of glycerol to glucose in media except 1% represents the carbon source is single carbon source glycerol, the concentration (m/v) of glycerol equal to or greater than the glucose (color figure online)

with appropriate ratio of glycerol to glucose could supply better precursors and NADPH than single carbon source for astaxanthin biosynthesis.

Discussion

The regulation of heterologous biosynthetic pathways is a recurrent theme in metabolic engineering, especially for the biosynthetic pathways of natural products. Thus, a simple method for effective combinatorial expression is important. Astaxanthin is an important natural pigment with extremely strong antioxidant activity which was reported to exceed those of β-carotene and α-tocopherol [15]. Recently, several engineered *E. coli* strains for astaxanthin biosynthesis were constructed through metabolic engineering. Examples include *E. coli* A1 (pFZ153) [25], *E. coli* ASTA-1 [23] and *E. coli* E/F [40]. To obtain these engineered strains, researchers adopted different strategies to optimize the expression levels of β-carotene hydroxylase and ketolase. Here, we combined β-carotene hydroxylases and ketolases from different sources within a single expression cassette to regulate astaxanthin production in *E. coli* through expression of artificial operons and fusion proteins. The yield of astaxanthin produced by strain ZF237T/$CrtZ_{As}$-$(GS)_1$-W_{Bs} was 127.6% and 40.2% higher than that of strains ZF237T/$crtZ_{As}W_{Bs}$ and ZF237T/$crtZ_{Bs}W_{Ps}$, respectively. The production and intracellular content of astaxanthin produced by the best strain are comparable to the highest level in *E. coli* reported by other researchers after optimization of carbon source in shake flask.

Previous studies revealed that CrtZ from *Alcaligenes* sp. strain PC-1, *Paracoccus* sp. N81106 and *Brevundimonas* sp. SD212 have high zeaxanthin production efficiency from

β-carotene, while CrtW from *Brevundimonas* sp.SD212, *Paracoccus* sp. N81106 and *Nostoc* sp. PCC7120 showed high astaxanthin production efficiency in *E. coli* producing zeaxanthin [7, 8, 35]. However, the ZF237T-derived strains expressing the operons $crtZ_{As}W_{Ns}$, $crtZ_{Bs}W_{Ns}$, $crtZ_{Ps}W_{Ps}$, and $crtZ_{Ps}W_{Bs}$ did not accumulate detectable amounts of astaxanthin (Table 1). The results of qRT-PCR indicated that the operons $crtZ_{As}W_{Ns}$, $crtZ_{Bs}W_{Ns}$, $crtZ_{Ps}W_{Ps}$, and $crtZ_{Ps}W_{Bs}$ were expressed efficiently at the RNA level (Fig. S1), yet the strains did not accumulate detectable amount of astaxanthin and we failed to relate the relative transcription levels to astaxanthin accumulation. However, we found that the total relative transcriptional levels of genes *crtZ* and *crtW* within the four operons either too low or too high compared with the other five operons, such as $crtZ_{As}W_{Ns}$ to $crtZ_{As}W_{Bs}$ and $crtZ_{Ps}W_{Ps}$ to $crtZ_{Ps}W_{Ns}$. We speculated this possibly affected the enzyme activities. Another possible reason is the competition for common substrates between the CrtZ and CrtW enzymes due to their broad substrate spectra and different affinity for the metabolites in vivo [29]. In addition, we noted that strains ZF237T/$crtZ_{As}W_{Ns}$ and ZF237T/$crtZ_{Bs}W_{Ns}$ did not accumulated detectable amounts of astaxanthin while strain ZF237T/$crtZ_{Ps}W_{Ns}$ accumulated 1.67 mg/L of astaxanthin (Table 1 and Fig. 2b). qRT-PCR showed that the total relative transcriptional of genes *crtZ* and *crtW* within operons $crtZ_{As}W_{Ns}$ and $crtZ_{Bs}W_{Ns}$ were lower than that of operon $crtZ_{Ps}W_{Ns}$ (Fig. S1). The exact reason for these failure merits further investigation in the future.

Park et al. fused eight tags to the N- or C-terminus of the trCrBKT membrane protein and screened two signal peptides, OmpF and TrxA, which could enhance the production of astaxanthin 2.08-fold compared to that obtained without a tag [32]. Ye et al. linked CrtW and CrtZ using a fexible eight-amino acids linker and targeted the fusion to membrane via a GlpF protein fusion in *E. coli*, and the production of astaxanthin was increased by 215.4% after optimal localization configuration [38]. We fused CrtZ and CrtW based on our operons directly or via peptide linkers. We found that the ZF237T-derived strains expressing fusion proteins with CrtZ attached to the N-terminus accumulated much more astaxanthin than the strains expressing fusion proteins with CrtW attached to the N-terminus, and most of the ZF237T-derived strains harboring $CrtW_{Bs}$-Z_{As} fusion proteins did not accumulate astaxanthin after introducing peptide linkers (Table S4). This phenomenon was similar to the research just reported by Nogueira et al. [31]. We inferred that the arrangement of modules within fusion proteins has a significant influence on their conformations and further affects their activities. Therefore, I-TASSER protein structure predictor was used to produce homology models of the fusion proteins $CrtZ_{As}$-W_{Bs} and $CrtW_{Bs}$-Z_{As}, because the astaxanthin production of strain ZF237T/$CrtZ_{As}$-W_{Bs} was 58.5% higher than that of strain ZF237T/$crtZ_{As}W_{Bs}$ while strain ZF237T/$CrtW_{Bs}$-Z_{As} only produced an amount equivalent to 11.67% of strain ZF237T/$crtZ_{As}W_{Bs}$. Sequence analysis revealed that CrtZ from *Alcaligenes* sp. strain PC-1 and CrtW from *Brevundimonas* sp. SD212 both have several conserved histidine motifs (HX_4H, HX_2HH or HHXHH), four in $CrtZ_{As}$ and three in $CrtW_{Bs}$ (Fig. 5a). These motifs are Fe^{2+} binding sites and are also characteristic of membrane-associated fatty acid desaturases and sterol desaturases [8, 10]. Functional characterization of β-carotene hydroxylase and mutational analysis of β-carotene ketolase demonstrated that these motifs are indispensable for their activities [4, 39]. Considering that topology models of conserved histidine motifs were available [4, 39], we concentrated our analysis on the changes of the locations of the histidine motifs in the two fusion proteins. First, we established the models of the proteins $CrtZ_{As}$ and $CrtW_{Bs}$ and found that the simulated structures of $CrtZ_{As}$ and $CrtW_{Bs}$ resemble that of a cone frustum which is composed of an α helix and an aperiodical coil. The conserved histidine motifs of the two enzymes were adjacent to each other at the bottom of the cone frustum, and the secondary structures of the histidine motifs were α-helical except for the histidine motif HDGLVH of $CrtZ_{As}$, which was an aperiodical coil (Fig. 5b). The two models were consistent with the topology models and prediction of 3D structures reported previously [4, 31, 39]. Second, in view of astaxanthin production, it was conceivable that the locations of the histidine motifs were different in the structures of the fusion proteins $CrtZ_{As}$-W_{Bs} and $CrtW_{Bs}$-Z_{As}. Indeed, structure modeling showed that the fusion protein $CrtZ_{As}$-W_{Bs} formed an oblique cylinder while the shape of $CrtW_{Bs}$-Z_{As} was cylindrical, and the hisidine motifs were distributed in different parts of the two cylinders. The surface structure analysis showed that all the histidine motifs were on the surface of the $CrtZ_{As}$-W_{Bs} fusion proteins, whereas the three histidine motifs (HHEHH of $CrtZ_{As}$, HDGLVH and HRLHH of $CrtW_{Bs}$) were inside the fusion protein $CrtW_{Bs}$-Z_{As} (Fig. S2). Therefore, our structure analysis showed that the differences in locations between the two fusion protein formats may affect the enzyme activity and substrate preference. Certainly, we had no information about the active sites of enzymes $CrtZ_{As}$ and $CrtW_{Bs}$, molecular docking could be used to identity the active sites of the two enzymes, and investigate the changes of physical distance between the sites in fusion proteins in the future. In addition, enzyme kinetics should be adopted to investigate the activities of the fusion proteins $CrtZ_{As}$-W_{Bs} and $CrtW_{Bs}$-Z_{As}.

Different peptide linkers are always used to create different fusion proteins because the nature of linker significantly affects the correct folding and activity of fusion protein [1]. Glycine has the simplest structure, minimum molecular weight and best flexibility compared to other 19 amino acids. Serine is the most hydrophilic polar amino acid. The

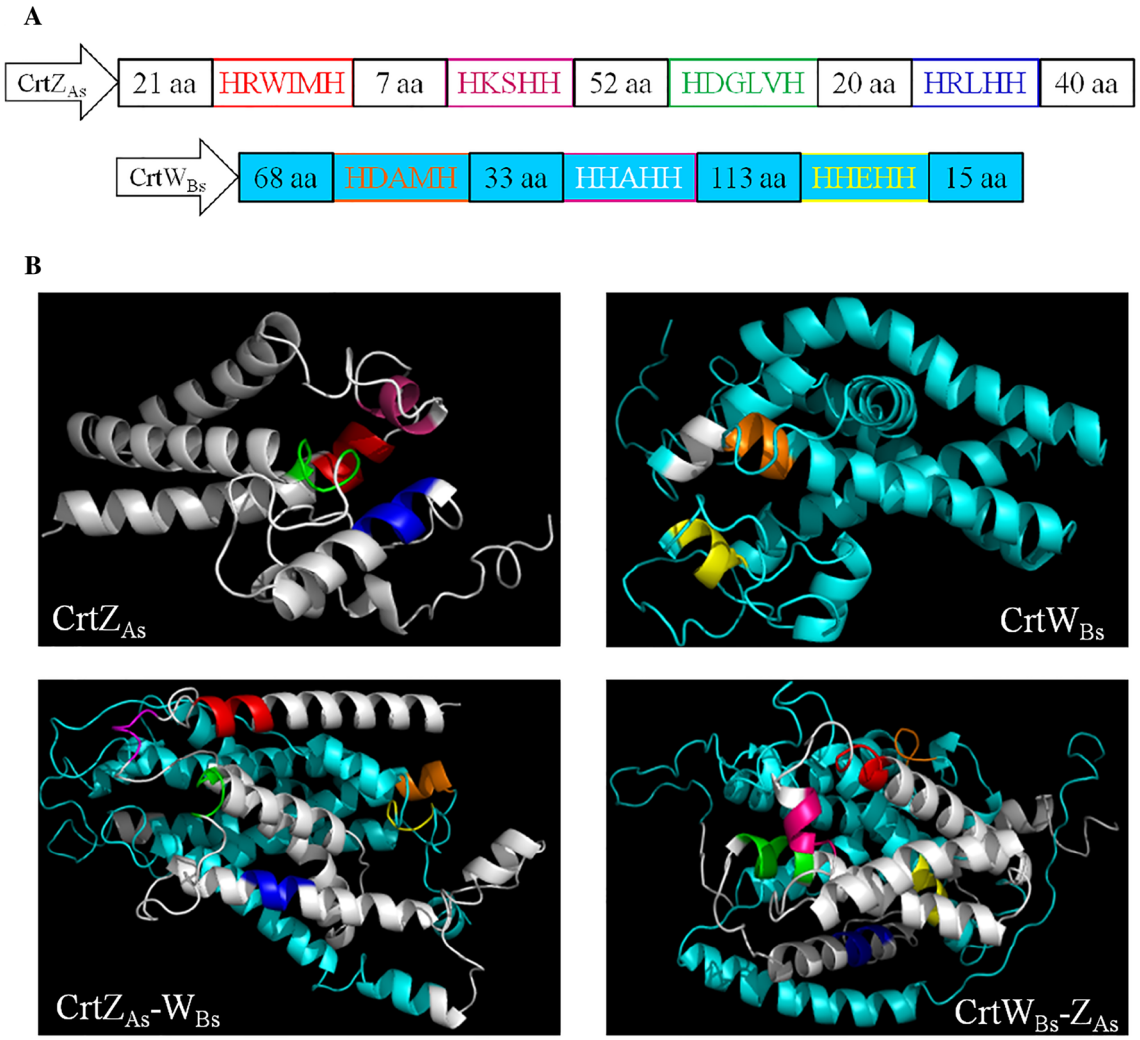

Fig. 5 Homology based models $CrtZ_{As}$, $CrtW_{Bs}$, $CrtZ_{As}$-W_{Bs} and $CrtW_{Bs}$-Z_{As}. **a** The histidine motifs of CrtZ from *Alcaligenes* sp. strain PC-1 and CrtW from *Brevundimonas* sp. SD212 were highlighted in uppercase letter with different colors. **b** Structure-based homology models of $CrtZ_{As}$, $CrtW_{Bs}$ and fusion proteins. The colors of histidine motifs correspond to the colors of the capital letter in **a** (color figure online)

incorporation of Gly and Ser can maintain the flexibility and the stability of linker in aqueous solution [6]. The production of astaxanthin was significantly different among the ZF237T-derived strains expressing $CrtZ_{As}$-W_{Bs} fusion proteins, with the highest value being 21-fold higher than the lowest. In addition, we noted that the accumulated amounts of lycopene and β-carotene were different among these strains. The lycopene and β-carotene production of the ZF237T-derived strains harboring fusion proteins with GSG linkers was higher than with GS linkers (Fig. 3c). These results indicated that the length and composition of the peptide linkers not only influenced the activities of the fusion proteins but also the metabolic fluxes in carotenoid biosynthesis. This was consistent with previous reports that the linker length and composition greatly affect the production of patchoulol, resveratrol and astaxanthin [1, 12, 31]. In attempt to explore the reasons, we produced homology models of fusion proteins $CrtZ_{As}$-$(GS)_2$-W_{Bs} and $CrtZ_{As}$-$(GSG)_2$-W_{Bs} via I-TASSER protein structure predictor because the strains expressing the two fusions accumulated similar amount of astaxanthin but different amounts of β-carotene and lycopene (Fig. 3b, c). The models showed that the secondary structure of histine motif HHEHH in fusion $CrtZ_{As}$-$(GS)_2$-W_{Bs} was aperiodical while it was α helix in fusion $CrtZ_{As}$-$(GSG)_2$-W_{Bs} (Fig. S3). In addition, we found that $(GS)_2$ linker located inside of the fusion $CrtZ_{As}$-$(GS)_2$-W_{Bs} and $(GSG)_2$ linker located outside of the fusion $CrtZ_{As}$-$(GSG)_2$-W_{Bs} (Fig. S3). We inferred these changes caused the different activities of the two fusions and thus affected the flux for astaxanthin biosynthesis.

The biosynthetic pathways of natural products often contain bi-functional enzymes and regulatory elements. To

construct cell factories for the industrial manufactory of natural products, these bio-bricks must be first assembled into one or more operons and then optimized. Here, we succeeded in regulating the production of astaxanthin in vivo by combining the expression of different oxygenases. Our observations provide a reference for the construction and regulation of other pathways comprising bi- or even multi-functional enzymes.

Funding This work was supported by the National Natural Science Foundation of China (NSFC-21621004, NSFC-21776208 and NSFC-21776209).

Compliance with ethical standards

Conflict of interest The authors declare that they have no conflict of interest.

Ethical approval This article does not contain any studies with human participants performed by any of the authors.

References

1. Albertsen L, Chen Y, Bach LS, Rattleff S, Maury J, Brix S, Nielsen J, Mortensen UH (2011) Diversion of flux toward sesquiterpene production in *saccharomyces cerevisiae* by fusion of host and heterologous enzymes. Appl Environ Microbiol 77:1033–1040. https://doi.org/10.1128/aem.01361-10
2. Alcaíno J, Barahona S, Carmona M, Lozano C, Marcoleta A, Niklitschek M, Sepúlveda D, Baeza M, Cifuentes V (2008) Cloning of the cytochrome p450 reductase (*crtR*) gene and its involvement in the astaxanthin biosynthesis of *Xanthophyllomyces dendrorhous*. BMC Microbiol 8:169. https://doi.org/10.1186/1471-2180-8-169
3. Biggs BW, Lim CG, Sagliani K, Shankar S, Stephanopoulos G, De Mey M, Ajikumar PK (2016) Overcoming heterologous protein interdependency to optimize P450-mediated taxol precursor synthesis in *Escherichia coli*. Proc Natl Acad Sci 113:3209
4. Bouvier F, Keller Y, d'Harlingue A, Camara B (1998) Xanthophyll biosynthesis: molecular and functional characterization of carotenoid hydroxylases from pepper fruits (*Capsicum annuum* L.). Biochim Biophys Acta 1391:320–328. https://doi.org/10.1016/S0005-2760(98)00029-0
5. Chang MCY, Eachus RA, Trieu W, Ro D-K, Keasling JD (2007) Engineering *Escherichia coli* for production of functionalized terpenoids using plant P450s. Nat Chem Biol 3:274. https://doi.org/10.1038/nchembio875
6. Chen X, Zaro JL, Shen W-C (2013) Fusion protein linkers: property, design and functionality. Adv Drug Deliver Rev 65:1357–1369. https://doi.org/10.1016/j.addr.2012.09.039
7. Choi S-K, Matsuda S, Hoshino T, Peng X, Misawa N (2006) Characterization of bacterial β-carotene 3,3′-hydroxylases, CrtZ, and P450 in astaxanthin biosynthetic pathway and adonirubin production by gene combination in *Escherichia coli*. Appl Microbiol Biotechnol 72:1238. https://doi.org/10.1007/s00253-006-0426-2
8. Choi S-k, Nishida Y, Matsuda S, Adachi K, Kasai H, Peng X, Komemushi S, Miki W, Misawa N (2005) Characterization of β-carotene ketolases, CrtW, from marine bacteria by complementation analysis in *Escherichia coli*. Mar Biotechnol 7:515–522. https://doi.org/10.1007/s10126-004-5100-z
9. Durnin G, Clomburg J, Yeates Z, Alvarez PJJ, Zygourakis K, Campbell P, Gonzalez R (2009) Understanding and harnessing the microaerobic metabolism of glycerol in *Escherichia coli*. Biotechnol Bioeng 103:148–161. https://doi.org/10.1002/bit.22246
10. Fraser PD, Miura Y, Misawa N (1997) In vitro characterization of astaxanthin biosynthetic enzymes. J Biol Chem 272:6128–6135. https://doi.org/10.1074/jbc.272.10.6128
11. Fraser PD, Shimada H, Misawa N (1998) Enzymic confirmation of reactions involved in routes to astaxanthin formation, elucidated using a direct substrate in vitro assay. Eur J Biochem 252:229–236. https://doi.org/10.1046/j.1432-1327.1998.2520229.x
12. Guo H, Yang Y, Xue F, Zhang H, Huang T, Liu W, Liu H, Zhang F, Yang M, Liu C, Lu H, Zhang Y, Ma L (2017) Effect of flexible linker length on the activity of fusion protein 4-coumaroyl-CoA ligase:stilbene synthase. Mol BioSyst 13:598–606. https://doi.org/10.1039/C6MB00563B
13. Heckman KL, Pease LR (2007) Gene splicing and mutagenesis by PCR-driven overlap extension. Nat Protoc 2:924. https://doi.org/10.1038/nprot.2007.132
14. Henke N, Heider S, Peters-Wendisch P, Wendisch V (2016) Production of the marine carotenoid astaxanthin by metabolically engineered *Corynebacterium glutamicum*. Mar Drugs 14:124
15. Higuera-Ciapara I, Félix-Valenzuela L, Goycoolea FM (2006) Astaxanthin: a review of its chemistry and applications. Crit Rev Food Sci 46:185–196. https://doi.org/10.1080/10408690590957188
16. Jin J, Wang Y, Yao M, Gu X, Li B, Liu H, Ding M, Xiao W, Yuan Y (2018) Astaxanthin overproduction in yeast by strain engineering and new gene target uncovering. Biotechnol Biofuels 11:230. https://doi.org/10.1186/s13068-018-1227-4
17. Jin W, Xu X, Jiang L, Zhang Z, Li S, Huang H (2015) Putative carotenoid genes expressed under the regulation of Shine-Dalgarno regions in *Escherichia coli* for efficient lycopene production. Biotechnol Lett 37:2303–2310. https://doi.org/10.1007/s10529-015-1922-1
18. Kosuri S, Goodman DB, Cambray G, Mutalik VK, Gao Y, Arkin AP, Endy D, Church GM (2013) Composability of regulatory sequences controlling transcription and translation in *Escherichia coli*. Proc Natl Acad Sci 110:14024
19. Li G, Huang Z, Zhang C, Dong B-J, Guo R-H, Yue H-W, Yan L-T, Xing X-H (2016) Construction of a linker library with widely controllable flexibility for fusion protein design. Appl Microbiol Biotechnol 100:215–225. https://doi.org/10.1007/s00253-015-6985-3
20. Li Y, Lin Z, Huang C, Zhang Y, Wang Z, Tang Y-j, Chen T, Zhao X (2015) Metabolic engineering of *Escherichia coli* using CRISPR–Cas9 meditated genome editing. Metab Eng 31:13–21. https://doi.org/10.1016/j.ymben.2015.06.006
21. Lin Z, Xu Z, Li Y, Wang Z, Chen T, Zhao X (2014) Metabolic engineering of *Escherichia coli* for the production of riboflavin. Microb Cell Fact 13:104. https://doi.org/10.1186/s12934-014-0104-5
22. Livak KJ, Schmittgen TD (2001) Analysis of relative gene expression data using real-time quantitative PCR and the $2^{-\Delta\Delta CT}$ method. Methods 25:402–408. https://doi.org/10.1006/meth.2001.1262
23. Lu Q, Bu Y-F, Liu J-Z (2017) Metabolic engineering of *Escherichia coli* for producing astaxanthin as the predominant carotenoid. Mar Drugs 15:296
24. Lv X, Xu H, Yu H (2013) Significantly enhanced production of isoprene by ordered coexpression of genes *dxs*, *dxr*, and *idi* in *Escherichia coli*. Appl Microbiol Biotechnol 97:2357–2365. https://doi.org/10.1007/s00253-012-4485-2
25. Ma T, Zhou Y, Li X, Zhu F, Cheng Y, Liu Y, Deng Z, Liu T (2015) Genome mining of astaxanthin biosynthetic genes from *Sphingomonas* sp. ATCC 55669 for heterologous overproduction

in *Escherichia coli*. Biotechnol J 11:228–237. https://doi.org/10.1002/biot.201400827
26. Martín JF, Gudiña E, Barredo JL (2008) Conversion of β-carotene into astaxanthin: two separate enzymes or a bifunctional hydroxylase-ketolase protein? Microb Cell Fact 7:3. https://doi.org/10.1186/1475-2859-7-3
27. Martínez K, de Anda R, Hernández G, Escalante A, Gosset G, Ramírez OT, Bolívar FG (2008) Coutilization of glucose and glycerol enhances the production of aromatic compounds in an *Escherichia coli* strain lacking the phosphoenolpyruvate: carbohydrate phosphotransferase system. Microb Cell Fact 7:1. https://doi.org/10.1186/1475-2859-7-1
28. Misawa N, Satomi Y, Kondo K, Yokoyama A, Kajiwara S, Saito T, Ohtani T, Miki W (1995) Structure and functional analysis of a marine bacterial carotenoid biosynthesis gene cluster and astaxanthin biosynthetic pathway proposed at the gene level. J Bacteriol 177:6575–6584. https://doi.org/10.1128/jb.177.22.6575-6584.1995
29. Misawa N, Shimada H (1998) Metabolic engineering for the production of carotenoids in non-carotenogenic bacteria and yeasts. J Biotechnol 59:169–181. https://doi.org/10.1016/S0168-1656(97)00154-5
30. Nishida Y, Adachi K, Kasai H, Shizuri Y, Shindo K, Sawabe A, Komemushi S, Miki W, Misawa N (2005) Elucidation of a carotenoid biosynthesis gene cluster encoding a novel enzyme, 2,2′-β-hydroxylase, from *Brevundimonas* sp. strain SD212 and combinatorial biosynthesis of new or rare xanthophylls. Appl Environ Microbiol 71:4286
31. Nogueira M, Enfissi EMA, Welsch R, Beyer P, Zurbriggen MD, Fraser PD (2019) Construction of a fusion enzyme for astaxanthin formation and its characterisation in microbial and plant hosts: a new tool for engineering ketocarotenoids. Metab Eng 52:243–252. https://doi.org/10.1016/j.ymben.2018.12.006
32. Park SY, Binkley RM, Kim WJ, Lee MH, Lee SY (2018) Metabolic engineering of *Escherichia coli* for high-level astaxanthin production with high productivity. Metab Eng 49:105–115. https://doi.org/10.1016/j.ymben.2018.08.002
33. Roy A, Kucukural A, Zhang Y (2010) I-TASSER: a unified platform for automated protein structure and function prediction. Nat Protoc 5:725. https://doi.org/10.1038/nprot.2010.5
34. Russell DW, Sambrook J (2001) Molecular cloning: a laboratory manual. Cold Spring Harbor, Cold Spring Harbor Laboratory
35. Scaife MA, Burja AM, Wright PC (2009) Characterization of cyanobacterial β-carotene ketolase and hydroxylase genes in *Escherichia coli*, and their application for astaxanthin biosynthesis. Biotechnol Bioeng 103:944–955. https://doi.org/10.1002/bit.22330
36. Scaife MA, Ma CA, Ninlayarn T, Wright PC, Armenta RE (2012) Comparative analysis of β-carotene hydroxylase genes for astaxanthin biosynthesis. J Nat Prod 75:1117–1124. https://doi.org/10.1021/np300136t
37. Yang J, Zhang Y (2015) I-TASSER server: new development for protein structure and function predictions. Nucleic Acids Res 43:W174–W181. https://doi.org/10.1093/nar/gkv342
38. Ye L, Zhu X, Wu T, Wang W, Zhao D, Bi C, Zhang X (2018) Optimizing the localization of astaxanthin enzymes for improved productivity. Biotechnol Biofuels 11:278. https://doi.org/10.1186/s13068-018-1270-1
39. Ye RW, Stead KJ, Yao H, He H (2006) Mutational and functional analysis of the β-carotene ketolase involved in the production of canthaxanthin and astaxanthin. Appl Environ Microbiol 72:5829
40. Zhang C, Seow VY, Chen X, Too H-P (2018) Multidimensional heuristic process for high-yield production of astaxanthin and fragrance molecules in *Escherichia coli*. Nat Commun 9:1858. https://doi.org/10.1038/s41467-018-04211-x
41. Zhou P, Xie W, Li A, Wang F, Yao Z, Bian Q, Zhu Y, Yu H, Ye L (2017) Alleviation of metabolic bottleneck by combinatorial engineering enhanced astaxanthin synthesis in *Saccharomyces cerevisiae*. Enzyme Microb Technol 100:28–36. https://doi.org/10.1016/j.enzmictec.2017.02.006
42. Zhou P, Ye L, Xie W, Lv X, Yu H (2015) Highly efficient biosynthesis of astaxanthin in *Saccharomyces cerevisiae* by integration and tuning of algal *crtZ* and *bkt*. Appl Microbiol Biotechnol 99:8419–8428. https://doi.org/10.1007/s00253-015-6791-y
43. Zhou YJ, Gao W, Rong Q, Jin G, Chu H, Liu W, Yang W, Zhu Z, Li G, Zhu G, Huang L, Zhao ZK (2012) Modular pathway engineering of diterpenoid synthases and the mevalonic acid pathway for miltiradiene production. J Am Chem Soc 134:3234–3241. https://doi.org/10.1021/ja2114486